

Quantitative atomic force microscopy

Hagen Söngen^{1,2}, Ralf Bechstein¹ and Angelika Kühnle¹

¹ Institute of Physical Chemistry, Johannes Gutenberg University Mainz, Duesbergweg 10-14, 55099 Mainz, Germany

² Graduate School Materials Science in Mainz, Staudinger Weg 9, 55128 Mainz, Germany

E-mail: soengen@uni-mainz.de, bechstein@uni-mainz.de and kuehnle@uni-mainz.de

Received 9 February 2017, revised 20 April 2017

Accepted for publication 26 April 2017

Published 6 June 2017



Abstract

A variety of atomic force microscopy (AFM) modes is employed in the field of surface science. The most prominent AFM modes include the amplitude modulation (AM) and the frequency modulation (FM) mode. Over the years, different ways for analyzing data acquired with different AFM modes have been developed, where each analysis is usually based on mode-specific assumptions and approximations. Checking the validity of the seemingly different approximations employed in the various analysis methods can be a tedious task. Moreover, a straightforward comparison of data analyzed with different methods can, therefore, be challenging. Here, we combine the existing evaluation methods which have been separately developed for the different AFM modes and present a unifying set of three equations. These three *AFM equations* allow for a straightforward analysis of AFM data within the *harmonic approximation*, regardless of the AFM mode. The three AFM equations provide the three and only pieces of information about the tip-sample force available within the harmonic approximation. We demonstrate the generality of our approach by quantitatively analyzing three-dimensional AFM data obtained in both the AM and FM mode.

Keywords: atomic force microscopy, quantitative analysis, operation mode


(Some figures may appear in colour only in the online journal)

1. Introduction

Three decades have passed since atomic force microscopy (AFM) has been invented [1]. During this time a number of experimental strategies for obtaining AFM data have been developed, namely static AFM as well as the dynamic AFM modes using ‘amplitude modulation’ [2] (AM), ‘phase modulation’ [3] (PM) and ‘frequency modulation’ [4] (FM). Numerous theoretical studies have been devoted to a quantitative understanding of the recorded AFM data in the respective modes. Each of these studies focuses on a specific operation mode, giving the impression that different approximations and specific theoretical treatment of AFM data is required for each AFM mode and different pieces of information about the tip-sample interaction are available in the different modes.

Here, based on existing theories that have been discussed in the view of specific modes only, we establish a comprehensive and generalized set of three equations that unifies the quantitative analysis of AFM data for the various AFM modes. We employ one approximation only, namely the *harmonic approximation*, which is equivalent to the perturbation approach by Giessibl [5, 6] and Dürig [7–10], the ‘Krylov–Bogoliubov averaging method’ by Sasaki and Tsukada *et al* [11–14], the Fourier expansion up to the first harmonic by Hölscher *et al* [15–17] and Ebeling and Hölscher [18] as well as the ‘method of slowly varying parameters’ [19] and others [20].

With AFM, the force between tip and sample is investigated. Observing the movement of the AFM tip allows to determine the tip-sample force. Within the harmonic approximation, the movement of the tip is approximated using three observables: the static deflection, the amplitude and the phase shift for a given excitation force amplitude and excitation frequency. Consequently, three pieces of information about the tip-sample force can be obtained, namely the average even

 Original content from this work may be used under the terms of the [Creative Commons Attribution 3.0 licence](https://creativecommons.org/licenses/by/3.0/). Any further distribution of this work must maintain attribution to the author(s) and the title of the work, journal citation and DOI.

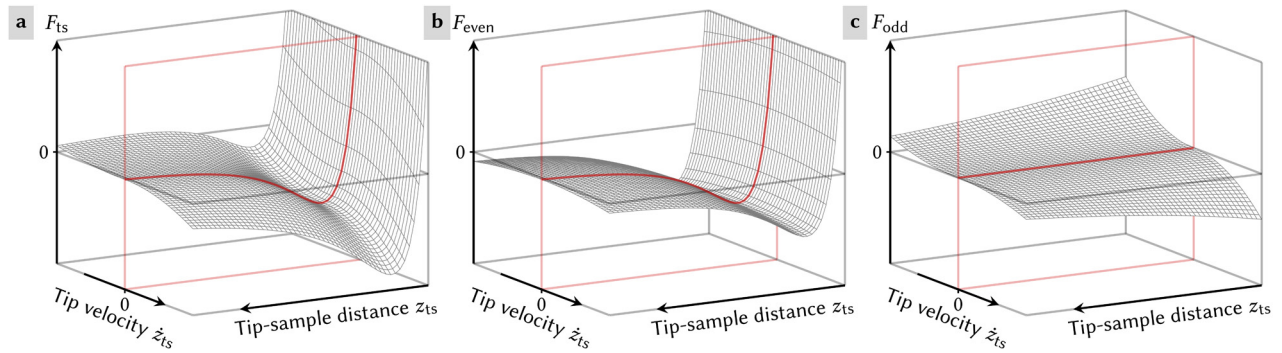


Figure 1. A tip-sample force F_{ts} and its components F_{even} and F_{odd} plotted as functions of the tip-sample distance and the tip velocity. Red curves indicate the static AFM case $\dot{z}_{ts} = 0$.

contribution to the tip-sample force, the average tip-sample force gradient and the average tip-sample damping constant. Here, we provide the three *AFM equations* which allow to obtain these three pieces of information. They are valid for analyzing AFM data irrespective of the specific AFM mode.

In the next section, we will derive the three AFM equations: first, we will split the tip-sample force into an even and an odd part. Second, we will introduce the path of the tip in the harmonic approximation. Third, we will analyze the average force acting on the tip, as well as the average kinetic energy and power. Finally, the three AFM equations will be obtained. They connect the quantities measured in AFM with the three and only pieces of information about the tip-sample force available in AFM within the harmonic approximation. We will discuss the physical meaning of the three obtained results in section 3. To demonstrate the applicability of the AFM equations, we have conducted three-dimensional (3D) AFM measurements above calcite (10.4) in pure water using both the AM and the FM mode. In section 4, we present the results of the quantitative analysis of both data sets.

2. Derivation of the three AFM equations

In atomic force microscopy, a sample is probed with a tip. The obtained AFM data provide a depiction of the sample based on the force acting on the tip caused by the sample, i.e. the tip-sample force \mathbf{F}_{ts} . In general, the tip-sample force has a component normal to the surface and components in the lateral directions. In this paper, we will only discuss the normal component of the tip-sample force F_{ts} and the resulting effect on the tip.

It appears plausible that the tip-sample force may in general depend on the tip-sample displacement $\mathbf{r}_{ts} = (x_{ts}, y_{ts}, z_{ts})$ and on the tip velocity $\dot{\mathbf{r}}_{ts}$. If the lateral tip displacement is constant ($x_{ts} = \text{const.}$ and $y_{ts} = \text{const.}$), it is interesting to study the normal component of the tip-sample force F_{ts} as function of both the tip-sample distance z_{ts} and the normal component of tip velocity \dot{z}_{ts} . A typical tip-sample force $F_{ts}(z_{ts}, \dot{z}_{ts})$ is drawn in figure 1(a). At zero velocity, i.e. in static AFM, a force-distance curve is obtained as indicated by the solid red line. This curve shows two prominent features which are typically observed: at large tip-sample distance, the tip-sample force approaches zero while the force increases sharply at small

distance. In dynamic AFM, the tip velocity is not zero at all times and, therefore, both the distance and velocity dependence of the tip-sample force is probed by the tip. A frictional force decelerates the tip. Accordingly, friction decreases the tip-sample force when the tip-sample distance is increasing, i.e. at positive tip velocity and *vice versa*.

It is always possible to split the tip-sample force into two terms F_{even} and F_{odd} : [10, 17, 21]

$$F_{ts}(z_{ts}, \dot{z}_{ts}) = F_{even}(z_{ts}, \dot{z}_{ts}) + F_{odd}(z_{ts}, \dot{z}_{ts}). \quad (1)$$

The term F_{even} describes the contribution to the tip-sample force that is *even* with respect to the tip velocity

$$F_{even}(z_{ts}, \dot{z}_{ts}) = F_{even}(z_{ts}, -\dot{z}_{ts}) \quad (2)$$

and the term F_{odd} describes the contribution to the tip-sample force that is *odd* with respect to the tip velocity

$$F_{odd}(z_{ts}, \dot{z}_{ts}) = -F_{odd}(z_{ts}, -\dot{z}_{ts}). \quad (3)$$

It is necessary to consider the even and odd components separately, since AFM can only extract these components of the tip-sample force [10, 17, 21], as already claimed in the introduction. We will later see that this is correct when we discuss the three AFM equations.

The even and odd contributions to the tip-sample force shown in figure 1(a) are depicted in figure 1(b) and (c), respectively. Since F_{ts} , F_{even} and F_{odd} can depend on the tip velocity, none of these quantities is in general a *unique* function of the tip-sample distance: At a given tip-sample distance, F_{ts} , F_{even} and F_{odd} can have different values depending on the tip velocity, as can be seen in figure 1.

For conducting an AFM experiment, the tip is mounted on the free end of a mechanical resonator which can be, e.g. a cantilever, a tuning fork or a length-extension sensor. This resonator is treated as a harmonic oscillator (see appendix B for the mathematical treatment), characterized by three properties: effective mass m , spring constant k and damping constant γ . Alternatively, the resonator can be characterized by its spring constant k , eigenfrequency $\nu_e = (2\pi)^{-1}\sqrt{k/m}$ and quality factor [22] $Q = \sqrt{km}/\gamma$. The other end of the resonator is fixed and the position of this fixed end with respect to the sample can be adjusted by a positioning system. Lateral positioning allows for obtaining AFM images and normal positioning allows for distance-dependent measurements.

The tip-sample distance is derived from measuring the deflection q of the free end of the resonator (see appendix A).

In a dynamic AFM experiment, the mechanical resonator is externally excited, e.g. by using a shake piezo or an excitation laser with an external excitation force according to $F_{\text{exc}} = F_0 \cos(2\pi\nu_{\text{exc}}t)$. The two excitation parameters excitation force amplitude F_0 and excitation frequency ν_{exc} are free to be picked by the experimentalist. Feedback loops can be optionally employed to adjust the excitation parameters during the experiment.

As a consequence of the excitation, the tip is moving. Observing the movement of the tip allows to determine the tip-sample force (see appendix C). Typically, however, the deflection q and the tip-sample distance z_{ts} are approximated by

$$\begin{aligned} q &= q_s + A \cos(2\pi\nu_{\text{exc}}t + \varphi) \\ z_{\text{ts}} &= z_c + A \cos(2\pi\nu_{\text{exc}}t + \varphi). \end{aligned} \quad (4)$$

In this case, the three observables static deflection q_s , amplitude A and phase shift φ are sufficient to describe the tip movement. Equation (4) is the *harmonic approximation*—the only approximation needed to derive the AFM equations. Its validity can be checked at any time during the experiment by analyzing the deflection, e.g. with an oscilloscope or a spectrum analyzer. The harmonic approximation (equation (4)) implies that the resonator is in steady state, i.e. F_0 , ν_{exc} , q_s , A , φ and the center position z_c are constant and the tip velocity is $\dot{z}_{\text{ts}} = \dot{q}$.

Several modes of conducting AFM experiments have been established. They differ in the number of employed feedback loops and their respective tasks. Figure 2 provides an overview starting in (a) with a static AFM experiment, in which no external excitation is applied and only the static deflection is observed. In dynamic AFM experiments both excitation parameters can be chosen to be constant (figure 2(b)). Alternatively, a feedback loop can be used to keep the amplitude constant by adjusting the excitation force amplitude (figure 2(c) and (e)). Another feedback loop can be used to keep the phase shift constant (usually at $-\pi/2$) by adjusting the excitation frequency (figure 2(d) and (e)). In all cases, another additional feedback loop can be employed to adjust the normal position of the fixed end of the resonator in order to keep one of the varying quantities at a predefined value. In all dynamic AFM experiments, the two excitation parameters F_0 and ν_{exc} as well as the three observables q_s , A and φ are necessary for a quantitative analysis. The three observables allow to extract in total three pieces of information about the tip-sample force. The connection between these three aspects of the tip-sample force and the three observables are stated in the three *AFM equations* as will be introduced in the following.

As a physically insightful way to derive the three AFM equations, we analyze the time-averaged force acting on the tip $\langle F \rangle_t$ as well as the average kinetic energy $\langle T \rangle_t$ of the resonator and the average power $\langle P \rangle_t$. The force $F = m\ddot{q}$ acting on the tip consists of four contributions: (1) the tip-sample

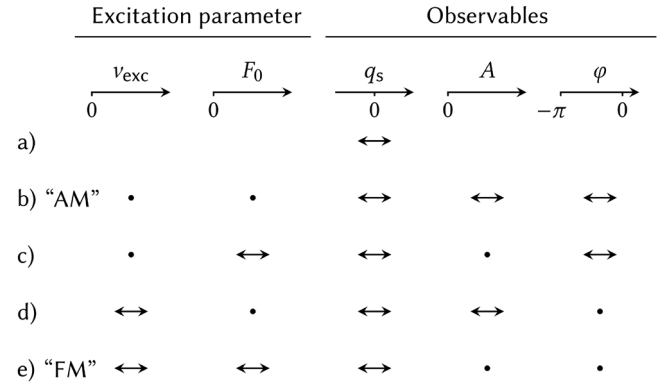


Figure 2. Overview of the static AFM mode (a) and the dynamic AFM modes (b)–(e). Points mark excitation parameters (F_0 , ν_{exc}) and observables (q_s , A , φ) that are held constant, double arrows indicate quantities that can change. The mode in (b) is usually referred to as amplitude-modulation AFM (AM-AFM) while (e) is known as frequency-modulation AFM (FM-AFM).

force, (2) the external excitation force, (3) the restoring force $-kq$ caused by the mechanical support keeping one end of the resonator in a fixed position and (4) the decelerating force $-\gamma\dot{q}$ caused by both internal friction in the moving resonator and friction of the resonator and tip moving through the surrounding medium:

$$F = m\ddot{q} = F_{\text{ts}}(z_{\text{ts}}, \dot{z}_{\text{ts}}) + F_0 \cos(2\pi\nu_{\text{exc}}t) - kq - \gamma\dot{q}. \quad (5)$$

The time average of the force acting on the tip is

$$\langle F \rangle_t = m \langle \ddot{q} \rangle_t \stackrel{(4)}{=} 0 \quad (6)$$

when the deflection is given by equation (4), as is indicated by the number above the equal sign. Inserting the tip-sample force (equation (1)) and the deflection (equation (4)) into equation (5) and averaging over time yields

$$\langle F \rangle_t = \langle F_{\text{even}}(z_{\text{ts}}, \dot{z}_{\text{ts}}) \rangle_t - kq_s \quad (7)$$

since $\langle F_{\text{odd}}(z_{\text{ts}}, \dot{z}_{\text{ts}}) \rangle_t = 0$. Combining the two equations (6) and (7) yields

$$\langle F_{\text{even}}(z_{\text{ts}}, \dot{z}_{\text{ts}}) \rangle_t = kq_s. \quad (8)$$

Knowing the spring constant of the resonator and measuring the static deflection allows to obtain the time average of the even contribution to the tip-sample force [23]. The time-averaged kinetic energy of the resonator is given by:

$$\langle T \rangle_t = \frac{m}{2} \langle \dot{z}_{\text{ts}}^2 \rangle_t \stackrel{(4)}{=} \frac{m}{4} (2\pi\nu_{\text{exc}})^2 A^2. \quad (9)$$

Another way to calculate the time-average of the kinetic energy is given by the virial theorem (VT):

$$\begin{aligned} \langle T \rangle_t &\stackrel{\text{(VT)}}{=} -\frac{1}{2} \langle F \cdot z_{\text{ts}} \rangle_t \stackrel{(4)}{=} -\frac{1}{2} \langle F \cdot (z_{\text{ts}} - z_c) \rangle_t \\ &\stackrel{(5)}{=} -\frac{1}{2} \langle F_{\text{even}}(z_{\text{ts}}, \dot{z}_{\text{ts}}) \cdot (z_{\text{ts}} - z_c) \rangle_t - \frac{F_0 A}{4} \cos \varphi + \frac{kA^2}{4}. \end{aligned} \quad (10)$$

From equations (9) and (10) it follows that:

$$\begin{aligned} & \langle F_{\text{even}}(z_{\text{ts}}, \dot{z}_{\text{ts}}) \cdot (z_{\text{ts}} - z_c) \rangle_t \\ &= \frac{kA^2}{2} - \frac{m}{2}(2\pi\nu_{\text{exc}})^2 A^2 - \frac{F_0 A}{2} \cos \varphi. \end{aligned} \quad (11)$$

The time-averaged power [24–26] is:

$$\langle P \rangle_t = \langle F \cdot \dot{z}_{\text{ts}} \rangle_t \stackrel{(4)}{=} 0 \quad (12)$$

when the deflection is given by equation (4). Using equation (5), the tip-sample force (equation (1)) and averaging over time yields

$$\begin{aligned} \langle P \rangle_t &= \langle F \cdot \dot{z}_{\text{ts}} \rangle_t \stackrel{(5)}{=} \langle F_{\text{odd}}(z_{\text{ts}}, \dot{z}_{\text{ts}}) \cdot \dot{z}_{\text{ts}} \rangle_t \\ &= \frac{F_0}{2}(2\pi\nu_{\text{exc}})A \sin \varphi - \frac{\gamma}{2}(2\pi\nu_{\text{exc}})^2 A^2. \end{aligned} \quad (13)$$

Inserting equation (12) in equation (13) results in

$$\langle F_{\text{odd}}(z_{\text{ts}}, \dot{z}_{\text{ts}}) \cdot \dot{z}_{\text{ts}} \rangle_t = \frac{F_0}{2}(2\pi\nu_{\text{exc}})A \sin \varphi + \frac{\gamma}{2}(2\pi\nu_{\text{exc}})^2 A^2. \quad (14)$$

The time-averaged force (equation (6)) and power (equation (12)) are both zero, which is in agreement with equation (4) describing the steady state. Only the even part of the tip-sample force contributes to the average kinetic energy (equation (10)), while only the odd part contributes to the average power (equation (13)) [10, 17, 21]. It will be discussed in section 3 that conservative tip-sample forces contribute to the even part, but non-conservative forces can, in general, contribute to both the even and the odd part.

In static AFM, a single piece of information about F_{ts} is gained from the measured static deflection according to the special case of equation (8): $F_{\text{even}}(z_{\text{ts}} = z_c, \dot{z}_{\text{ts}} = 0) = kq_s$. Since the velocity of the tip is zero, nothing can be learned about F_{odd} with static AFM.

In dynamic AFM the tip oscillates. In this case, the static deflection allows to assess the time-average of the even part of the tip-sample force according to equation (8). Moreover, dynamic AFM provides two more pieces of information about F_{ts} , namely the distance dependence of F_{even} and the velocity dependence of F_{odd} . To see that, we rearrange equations (11) and (14) in two steps. In the first step, the derivative of F_{even} is introduced as the tip-sample force gradient

$$k_{\text{ts}}(z_{\text{ts}}, \dot{z}_{\text{ts}}) = \frac{\partial F_{\text{even}}(z_{\text{ts}}, \dot{z}_{\text{ts}})}{\partial z_{\text{ts}}} \quad (15)$$

and F_{odd} is rewritten as the product of an even and an odd function [10, 19]

$$F_{\text{odd}}(z_{\text{ts}}, \dot{z}_{\text{ts}}) = -\gamma_{\text{ts}}(z_{\text{ts}}, \dot{z}_{\text{ts}}) \cdot \dot{z}_{\text{ts}}. \quad (16)$$

The obvious choice for the odd function is the tip velocity, the even function $\gamma_{\text{ts}}(z_{\text{ts}}, \dot{z}_{\text{ts}})$ is introduced as the tip-sample damping constant [17, 21]. In the second step, the time-averages in equation (8), (11) and (14) are expressed as weighted averages over the tip-sample distance (see appendix D for details):

$$\langle F_{\text{even}}(z_{\text{ts}}, \dot{z}_{\text{ts}}) \rangle_t = \langle F_{\text{even}}(z_{\text{ts}}, \dot{z}_{\text{ts}}) \rangle_{\cup} \quad (17)$$

$$\frac{2}{A^2} \langle F_{\text{even}}(z_{\text{ts}}, \dot{z}_{\text{ts}}) \cdot (z_{\text{ts}} - z_c) \rangle_t = \langle k_{\text{ts}}(z_{\text{ts}}, \dot{z}_{\text{ts}}) \rangle_{\cap} \quad (18)$$

$$-\frac{2}{(2\pi\nu_{\text{exc}})^2 A^2} \langle F_{\text{odd}}(z_{\text{ts}}, \dot{z}_{\text{ts}}) \cdot \dot{z}_{\text{ts}} \rangle_t = \langle \gamma_{\text{ts}}(z_{\text{ts}}, \dot{z}_{\text{ts}}) \rangle_{\cap} \quad (19)$$

Here, we use the weighted averages ‘cup’ (\cup) and ‘cap’ (\cap) according to

$$\langle f \rangle_{\cup} = \int_{-A}^A dz f(z_c + z) w_{\cup}(z), \quad w_{\cup}(z) = \frac{1}{\pi\sqrt{A^2 - z^2}} \quad (20)$$

$$\langle f \rangle_{\cap} = \int_{-A}^A dz f(z_c + z) w_{\cap}(z), \quad w_{\cap}(z) = \frac{2}{\pi A^2} \sqrt{A^2 - z^2} \quad (21)$$

with the positive and normalized weight functions w_{\cup} and w_{\cap} which average in the tip-sample distance interval $[z_c - A, z_c + A]$ around the center position of the tip z_c (see figure D1 in appendix D).

Finally, the three AFM equations are obtained from combining equations (8), (11) and (14) with equations (17)–(19)

$$\langle F_{\text{even}}(z_{\text{ts}}, \dot{z}_{\text{ts}}) \rangle_{\cup} = kq_s \quad (22)$$

$$\langle k_{\text{ts}}(z_{\text{ts}}, \dot{z}_{\text{ts}}) \rangle_{\cap} = k \left(1 - \left(\frac{\nu_{\text{exc}}}{\nu_e} \right)^2 \right) - \frac{F_0}{A} \cos \varphi \quad (23)$$

$$\langle \gamma_{\text{ts}}(z_{\text{ts}}, \dot{z}_{\text{ts}}) \rangle_{\cap} = -\frac{k}{2\pi\nu_e Q} - \frac{F_0}{2\pi\nu_{\text{exc}} A} \sin \varphi \quad (24)$$

using the eigenfrequency ν_e and the quality factor Q of the resonator. These are the three AFM equations, which allow to obtain the three pieces of information about the tip-sample force that are available within the harmonic approximation. The right-hand sides of the three AFM equations (22)–(24) are fully determined by the resonator properties k , ν_e and Q , the excitation parameters F_0 and ν_{exc} , and the observables q_s , A and φ . The three obtained quantities on the left-hand side are the average even part of the tip-sample force $\langle F_{\text{even}} \rangle_{\cup}$, the average tip-sample force gradient $\langle k_{\text{ts}} \rangle_{\cap}$ and the average tip-sample damping constant $\langle \gamma_{\text{ts}} \rangle_{\cap}$. Thus, in contrast to static AFM, where only the even tip-sample force contribution F_{even} can be obtained, dynamic AFM allows to additionally probe the distance dependence of F_{even} using $\langle k_{\text{ts}} \rangle_{\cap}$ as well as the velocity dependence of F_{odd} using $\langle \gamma_{\text{ts}} \rangle_{\cap}$. The three averages $\langle F_{\text{even}} \rangle_{\cup}$, $\langle k_{\text{ts}} \rangle_{\cap}$ and $\langle \gamma_{\text{ts}} \rangle_{\cap}$ are discussed in more detail in section 3.

The major advantage of the three AFM equations is that they hold true without restrictions to the experimental mode, as long as the harmonic approximation is valid. They can be applied, independent on how many feedback loops are used and irrespective of which of the five quantities discussed in figure 2 are held constant. Even in the case of poorly adjusted feedback loops, i.e. when all five quantities are varying to some extent, both excitation parameters (F_0 and ν_{exc}) and all

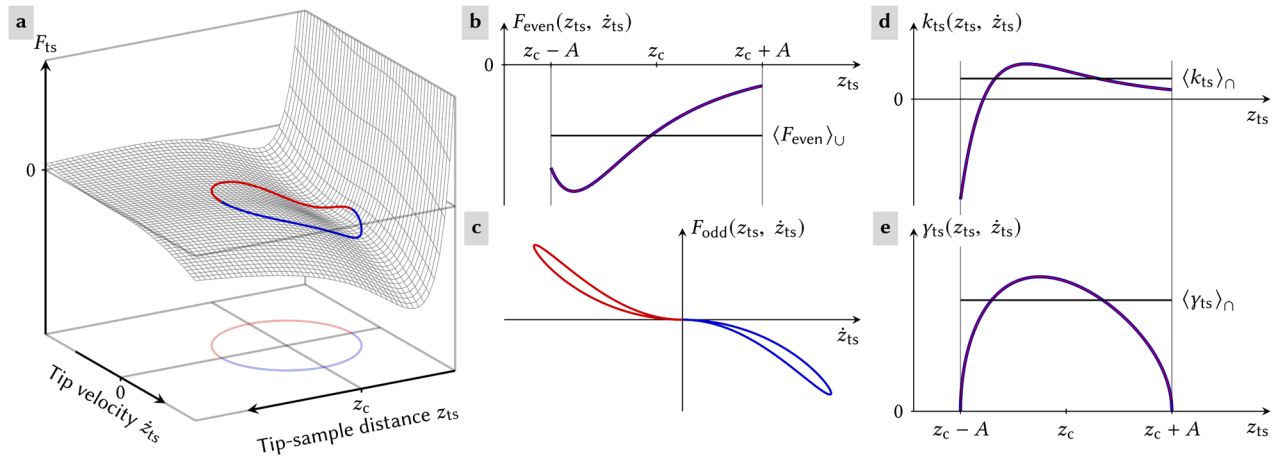


Figure 3. In (a) the tip-sample force as introduced in figure 1 is shown. The harmonic approximation (equation (4)) corresponds to a tip trajectory as indicated by the solid line (red—approach, blue—retract). In dynamic AFM, the tip-sample force is probed by the oscillating tip along this path. In static AFM, the tip-sample force at $z_{ts} = z_c$ and $\dot{z}_{ts} = 0$ is measured. The even and odd contribution to F_{ts} along the path of the tip are shown in (b) and (c). In (d) and (e), k_{ts} and γ_{ts} along the path of the tip are shown. The black horizontal lines in (b), (d) and (e) indicate the averages that can be obtained with the three AFM equations.

three observables (q_s , A and φ) are always experimentally accessible. Therefore, in all of these cases, AFM data can be analyzed quantitatively using the AFM equations, if all three observables and the excitation parameters are recorded. In the next section, we will discuss the three pieces of information that can be obtained with the three AFM equations (22)–(24).

3. The three pieces of information about the tip sample force

In this section, we discuss the physical meaning of the three quantities that can be obtained using the three AFM equations: the average even contribution of the tip sample force, the average tip-sample force gradient and the average tip-sample damping constant. Within the harmonic approximation, the tip probes the tip-sample force along the path described by equation (4) and indicated by the solid line in figure 3(a). The red line depicts the path of the approaching tip (negative tip velocity), the blue line the path of the retracting tip (positive tip velocity). Within one oscillation cycle, the tip probes the tip-sample force twice at each tip-sample distance—with a velocity that differs in its sign, but not in its absolute value.

In figure 3(b), F_{even} is plotted as a function of z_{ts} for the approaching (red) and retracting (blue) tip. According to equation (2), F_{even} is equal for the approaching and retracting tip along this path [16]. Consequently, the blue and red curve overlap. Within the harmonic approximation, F_{even} is a unique function of z_{ts} along a given path.

The other contribution to the tip-sample force is F_{odd} , which has an opposite sign for the approaching and retracting tip. This follows from equation (3) and can be recognized in figure 3(c), which shows F_{odd} as a function of the tip velocity. Even within the harmonic approximation, F_{odd} is not a unique function of z_{ts} .

The tip-sample force gradient k_{ts} and the tip-sample damping constant γ_{ts} are plotted in figure 3(d) and (e) as function of the tip-sample distance. Since both functions are even with respect to the tip velocity, they are unique functions of z_{ts} along a given path within the harmonic approximation.

The three AFM equations allow to obtain the average values of F_{even} , k_{ts} and γ_{ts} from the experimentally obtained observables q_s , A and φ and the excitation parameters F_0 and ν_{exc} . The first AFM equation (22) allows to determine the cup-average of the even force $\langle F_{\text{even}} \rangle_U$, which is indicated by the horizontal black line in figure 3(b). The time-average of the odd force is always zero as can be seen in figure 3(c). The weighted average of the tip-sample force gradient $\langle k_{ts} \rangle_O$ is the second piece of information about the tip-sample force that is available in dynamic AFM. It is obtained with the second AFM equation (23) and it is indicated by the horizontal black line in figure 3(d). The weighted average of the tip-sample damping constant $\langle \gamma_{ts} \rangle_O$ is the third piece of information about the tip-sample force that can be obtained from dynamic AFM data. The quantity is obtained with the third AFM equation (24) and is shown as a horizontal black line in figure 3(e).

It is straightforward to quantify the tip-sample interaction in terms of $\langle F_{\text{even}} \rangle_U$, $\langle k_{ts} \rangle_O$ and $\langle \gamma_{ts} \rangle_O$ using the AFM equations. Importantly, these three pieces of information about $F_{ts}(z_{ts}, \dot{z}_{ts})$ represent a complete description of the tip-sample force within the harmonic approximation (see appendix C). However, the average values might be a poor local description of F_{even} , k_{ts} and γ_{ts} , especially when large amplitudes are used in the experiment, i.e. when the average is performed over a large tip-sample distance range. In those cases it might be interesting to deconvolve $\langle F_{\text{even}} \rangle_U$, $\langle k_{ts} \rangle_O$ and $\langle \gamma_{ts} \rangle_O$, e.g. as suggested by Dürig [9], Giessibl [27] as well as Sader *et al* [28, 29] (see appendix D for a detailed description).

Obviously, it is possible to distinguish between *even* and *odd* contributions to the tip-sample force. Is it also possible to distinguish between the *conservative* and the *non-conservative* part of the tip-sample force? Any conservative force is necessarily independent of the tip velocity and, therefore, contributes solely to F_{even} . Any odd force has to be velocity-dependent and is, therefore, not conservative. In general, however, the even contribution is not necessarily purely conservative and the odd contribution does not necessarily contain all non-conservative contributions [21]. A simple example

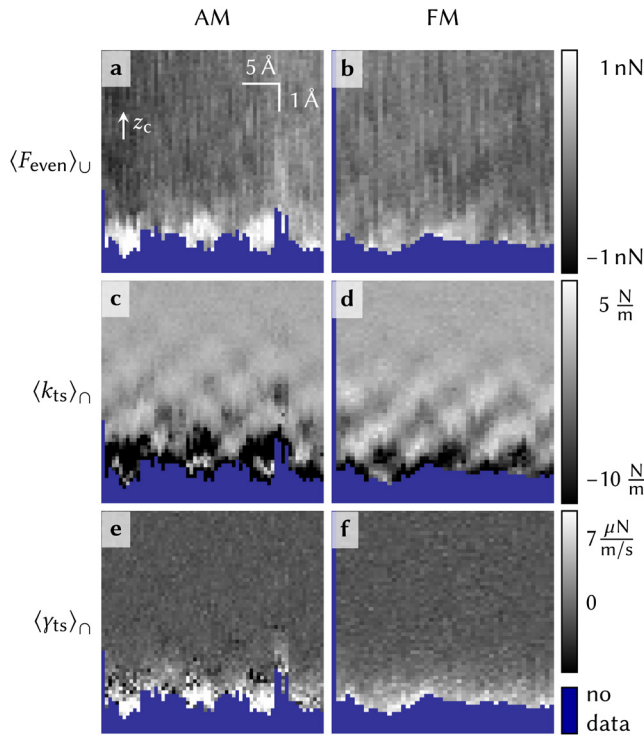


Figure 4. The three pieces of information about the tip-sample force, obtained with the three AFM equations (22)–(24). The 3D AFM data was obtained using the AM ((a), (c) and (e)) and the FM ((b), (d) and (f)) mode, respectively. The first row shows the average even force $\langle F_{\text{even}} \rangle_{\perp}$, the second row shows the average tip-sample force gradient $\langle k_{\text{ts}} \rangle_{\parallel}$ and the third row shows the average tip-sample damping constant $\langle \gamma_{\text{ts}} \rangle_{\parallel}$. Each frame is plotted in a way that the vertical axis corresponds to the center position of the tip oscillation z_c and the horizontal axis corresponds to a lateral tip-sample displacement along the $[48\bar{1}]$ direction on the calcite (10.4) surface. The color scales apply to both data within a row.

is a force contribution that we used in our plots of F_{ts} in figure 1 and 3: a force contribution that is proportional to $(\dot{z}_{\text{ts}})^2$ is not conservative, yet it contributes only to F_{even} and not to F_{odd} .

How can the experimentalist find out whether F_{even} is purely conservative? To answer this important question, it is certainly not enough to measure only the normal component of the tip-sample force. One feasible strategy might be to first exclude that F_{even} depends on the tip velocity. This can be done, for example by comparing the even force measured with static and dynamic AFM [30]. If F_{even} is independent of \dot{z}_{ts} it is possible that it is purely conservative. Second, the lateral components of the tip-sample force need to be calculated from analyzing the lateral movement of the tip. Only if the even part of the resulting tip-sample force field $\mathbf{F}_{\text{ts}}(\mathbf{r}_{\text{ts}})$ can be written as the negative gradient of a potential energy, the measured even force is purely conservative. In all other cases, it is dangerous to interpret the *even* part of F_{ts} as purely *conservative*, as pointed out in detail by Sader *et al* [21].

In the next section, we will demonstrate the applicability of the three AFM equations (22)–(24) by quantitatively analyzing AM-AFM and FM-AFM data.

4. Experimental demonstration

For demonstrating the applicability of the three AFM equations, we performed 3D AFM measurements at the calcite (10.4)-water interface [31–35]. We employed a setup [36–38] that allows to switch between the AM and FM mode (see figure 2) during the experiment to minimize changes at the tip and the sample (see appendix F for experimental details). In both modes, we simultaneously recorded all five channels of data: the two excitation parameters F_0 and ν_{exc} as well as the three observables q_s , A and φ . Using the three AFM equations, we computed the three quantities available from dynamic AFM data: the averaged even contribution to the tip-sample force $\langle F_{\text{even}} \rangle_{\perp}$, the averaged tip-sample force gradient $\langle k_{\text{ts}} \rangle_{\parallel}$ and the averaged tip-sample damping constant $\langle \gamma_{\text{ts}} \rangle_{\parallel}$.

Figure 4 shows these three pieces of information about the tip-sample force in a vertical slice through the 3D volume along the $[48\bar{1}]$ direction. The left and right column of figure 4 show the result of the quantitative analysis of AFM data obtained in AM- and FM-AFM measurements, respectively. Both sets of slices show the same features. For an interpretation of the observed patterns we refer the reader to [34] and [35]. The measured values for even force, force gradient and damping constant obtained from the AM and FM data sets are very similar. Of course they are not exactly the same, since the paths along which the averaging was done (equation (4)) were not exactly the same, as discussed in the previous sections. In appendix D we describe which further assumptions are necessary to deconvolve the averages using the approach by Sader *et al* [28, 29]. The description of their deconvolution method as well as the deconvolution of the data shown in figure 4(c) and (d) can be found in appendix D.

5. Conclusion

In this article we derived three AFM equations that can be universally applied to analyze AFM data. These three equations fully describe the tip-sample force regardless of the specific measurement mode (e.g. AM or FM-AFM) and even at poor feedback-loop performance—as long as the harmonic approximation is valid. As a result, raw data from any dynamic AFM experiment can always be related to three pieces of information about the tip-sample force: the average even force, the average tip-sample force gradient and the average tip-sample damping constant. We demonstrate the generality of the three AFM equations by analyzing 3D AFM data measured at the calcite (10.4)-water interface with AM- and FM-AFM.

Acknowledgments

We thank Frieder Mugele, Daniel Forchheimer, Amir F Payam, Laurent Nony and Christoph Marutschke for stimulating discussions. We are grateful to Philipp Rahe for critically reading the manuscript. We thank Michael Reichling and Clemens Barth for organizing the ‘German–French Summer

School on noncontact atomic force microscopy' which triggered many fruitful discussions.

HS is a recipient of a DFG-funded position through the Excellence Initiative (DFG/GSC 266). Financial support by the German Research Foundation (DFG) through Grant No. KU1980/7-1 is gratefully acknowledged.

Appendix A. Tip-sample distance and coordinate system

In general, the tip-sample force has a component normal to the surface and components in the lateral directions. As a consequence, the deflection of the resonator is affected in normal and lateral directions by the tip-sample force. We employ a coordinate system where the z -direction is oriented normal to the sample surface, pointing away from the sample. In this paper, we discuss only the normal component of the force acting on the tip and the resulting normal component of the deflection. The three-dimensional case reduces to a one-dimensional case with the normal components of the tip-sample force $F_{ts} = \mathbf{F}_{ts} \cdot \mathbf{e}_z$, the deflection $q = \mathbf{q} \cdot \mathbf{e}_z$ and the tip-sample distance $z_{ts} = \mathbf{r}_{ts} \cdot \mathbf{e}_z$, where \mathbf{e}_z is the unit vector in z .

It is desirable to obtain F_{ts} as a function of tip-sample distance z_{ts} . However, the tip-sample distance is experimentally not accessible. Instead, the deflection q is detected, and the *relative* displacement of the fixed end of the resonator with respect to the sample $\mathbf{r}_p = (x_p, y_p, z_p)$ can be adjusted with a positioning system, usually consisting of piezo elements. Obtaining the *absolute* tip-sample distance z_{ts} requires to know the distance z_0 between tip and sample when resonator and positioning system are in their respective rest positions ($q = 0$ and $z_p = 0$). The tip-sample distance is then given as $z_{ts} = z_0 + z_p + q$ and the center position of the tip is given as $z_c = z_0 + z_p + q_s$.

Appendix B. Transfer function of the harmonic oscillator

The aim of this section is to relate the resonator's deflection q to any excitation force. Any external excitation F_{exc} employed to drive the resonator and any tip-sample force $F_{ts}(z_{ts}, \dot{z}_{ts})$ excite the resonator and are, therefore, considered as excitation force. Applying the Fourier transform (\mathcal{F}) to equation (5) and using

$$\mathcal{F}[\dot{q}] = (2\pi\nu i) \mathcal{F}[q] \quad (\text{B.1})$$

$$\mathcal{F}[\ddot{q}] = (2\pi\nu i)^2 \mathcal{F}[q] \quad (\text{B.2})$$

leads to a linear relationship between the spectrum of the deflection $\mathcal{F}[q]$ and the spectrum of the excitation force

$$\mathcal{F}[q] = G_{ho}(\nu) \cdot \mathcal{F}[F_{ts}(z_{ts}, \dot{z}_{ts}) + F_{exc}] \quad (\text{B.3})$$

with the transfer function of the harmonic oscillator

$$G_{ho}(\nu) = \frac{1}{k - (2\pi\nu)^2 m + 2\pi\nu i \gamma} \quad (\text{B.4})$$

$$= \frac{1/k}{1 - \left(\frac{\nu}{\nu_e}\right)^2 + i \frac{\nu}{Q\nu_e}} \quad (\text{B.5})$$

$$= |G_{ho}(\nu)| \exp(i \varphi_{ho}(\nu)). \quad (\text{B.6})$$

The magnitude $|G_{ho}(\nu)|$ of the transfer function relates the magnitude of a spectral component of the excitation force with the magnitude of a spectral component of the deflection. Therefore, the function

$$|G_{ho}(\nu)| = \frac{1/k}{\sqrt{\left(1 - \left(\frac{\nu}{\nu_e}\right)^2\right)^2 + \left(\frac{\nu}{Q\nu_e}\right)^2}} \quad (\text{B.7})$$

is called *gain function*. The argument $\varphi_{ho}(\nu)$ of the transfer function of the harmonic oscillator relates the argument of a spectral component of the excitation force with the argument of a spectral component of the deflection. Therefore, the function $\varphi_{ho}(\nu)$ is called *phase shift function*. As the imaginary part of $G_{ho}(\nu)$ is equal to or less than zero, the phase shift function has values in the range of $-\pi \leq \varphi_{ho}(\nu) \leq 0$. The inversion of

$$\tan \varphi_{ho}(\nu) = -\frac{\nu}{Q\nu_e} / \left(1 - \left(\frac{\nu}{\nu_e}\right)^2\right) \quad (\text{B.8})$$

is therefore given by

$$\varphi_{ho}(\nu) = \begin{cases} \arctan\left(-\frac{\nu}{Q\nu_e} / \left(1 - \left(\frac{\nu}{\nu_e}\right)^2\right)\right) & 0 \leq \nu < \nu_e \\ -\pi/2 & \nu = \nu_e \\ -\pi + \arctan\left(-\frac{\nu}{Q\nu_e} / \left(1 - \left(\frac{\nu}{\nu_e}\right)^2\right)\right) & \nu > \nu_e \end{cases} \quad (\text{B.9})$$

or, alternatively, by using the *atan2* function, which takes the imaginary and real part of $G_{ho}(\nu)$ as two separate arguments:

$$\varphi_{ho}(\nu) = \text{atan2}\left(-\frac{\nu}{Q\nu_e}, 1 - \left(\frac{\nu}{\nu_e}\right)^2\right). \quad (\text{B.10})$$

Since $G_{ho}(\nu = 0) = 1/k$, any static excitation force F_s leads to a static deflection $q_s = F_s/k$. For $F_{ts} = 0$ and $F_{exc} = F_0 \cos(2\pi\nu_{exc}t)$, the deflection of the resonator is derived using equation (B.3) as

$$q = A \cos(2\pi\nu_{exc}t + \varphi) \quad (\text{B.11})$$

$$\text{with } A = |G_{ho}(\nu_{exc})| \cdot F_0 \quad (\text{B.12})$$

$$\text{and } \varphi = \varphi_{ho}(\nu_{exc}). \quad (\text{B.13})$$

Note that $|G_{ho}(\nu = \nu_e)| = Q/k = Q |G_{ho}(\nu = 0)|$.

Appendix C. Fourier series

In the manuscript, we rely on the harmonic approximation to derive the three AFM equations. In this section, we show

the connection between the harmonic approximation and the expansion of the tip-sample force and the deflection as Fourier series. The tip-sample force F_{ts} can be any function of the tip-sample distance z_{ts} and of the tip velocity \dot{z}_{ts} as illustrated in figure 3(a). The tip is moving and, therefore, senses the tip-sample force along a certain path through the tip-sample force landscape. Consequently, F_{ts} becomes a function of time. The tip-sample force which is sensed by the tip changes the way the tip is moving. The path and the force which is sensed along that path are connected according to equation (B.3).

Assuming $F_{\text{ts}}(t)$ and $q(t)$ are periodic functions in time with a period of $1/\nu_{\text{exc}}$, they can be expressed using the following Fourier series:

$$F_{\text{ts}}(t) = F_{\text{even}}^{(0)} + \sum_{n=1}^{\infty} (F_{\text{even}}^{(n)} \cos(2\pi n \nu_{\text{exc}} t + \varphi) + F_{\text{odd}}^{(n)} \sin(2\pi n \nu_{\text{exc}} t + \varphi)) \quad (\text{C.1})$$

$$q(t) = q_s + A \cos(2\pi \nu_{\text{exc}} t + \varphi) + \sum_{n=2}^{\infty} A^{(n)} \cos(2\pi n \nu_{\text{exc}} t + \varphi^{(n)}). \quad (\text{C.2})$$

The Fourier coefficients of F_{ts} are obtained according to

$$F_{\text{even}}^{(0)} = \langle F_{\text{ts}} \rangle_t = \langle F_{\text{even}} \rangle_t \quad (\text{C.3})$$

$$F_{\text{even}}^{(n)} = 2 \langle F_{\text{ts}} \cos(2\pi n \nu_{\text{exc}} t + \varphi) \rangle_t = 2 \langle F_{\text{even}} \cos(2\pi n \nu_{\text{exc}} t + \varphi) \rangle_t \quad (\text{C.4})$$

$$F_{\text{odd}}^{(n)} = 2 \langle F_{\text{ts}} \sin(2\pi n \nu_{\text{exc}} t + \varphi) \rangle_t = 2 \langle F_{\text{odd}} \sin(2\pi n \nu_{\text{exc}} t + \varphi) \rangle_t. \quad (\text{C.5})$$

Employing equation (5), the Fourier coefficients describing the constant force and the first harmonic ($n = 1$) are

$$F_{\text{even}}^{(0)} = \langle F_{\text{even}} \rangle_t = k q_s \quad (\text{C.6})$$

$$F_{\text{even}}^{(1)} = \frac{2}{A} \langle F_{\text{even}} \cdot (z_{\text{ts}} - z_c) \rangle_t = k A \left(1 - \left(\frac{\nu_{\text{exc}}}{\nu_e} \right)^2 \right) - F_0 \cos \varphi \quad (\text{C.7})$$

$$F_{\text{odd}}^{(1)} = \frac{2 \langle F_{\text{odd}} \cdot \dot{z}_{\text{ts}} \rangle_t}{-2\pi \nu_{\text{exc}} A} = -k A \left(\frac{\nu_{\text{exc}}}{Q \nu_e} \right) - F_0 \sin \varphi. \quad (\text{C.8})$$

The higher harmonics ($n > 1$) are described by

$$F_{\text{even}}^{(n)} = k A^{(n)} \left(\left(1 - \left(\frac{n \nu_{\text{exc}}}{\nu_e} \right)^2 \right) \cos(\varphi - \varphi^{(n)}) + \left(\frac{n \nu_{\text{exc}}}{Q \nu_e} \right) \sin(\varphi - \varphi^{(n)}) \right) \quad (\text{C.9})$$

$$F_{\text{odd}}^{(n)} = k A^{(n)} \left(\left(1 - \left(\frac{n \nu_{\text{exc}}}{\nu_e} \right)^2 \right) \sin(\varphi - \varphi^{(n)}) - \left(\frac{n \nu_{\text{exc}}}{Q \nu_e} \right) \cos(\varphi - \varphi^{(n)}) \right). \quad (\text{C.10})$$

In case the amplitude $A^{(n)}$ and the phase shift $\varphi^{(n)}$ of a harmonic of the deflection are available from the experiment, the corresponding Fourier coefficient of F_{ts} can be obtained using equations (C.6)–(C.10). However, it is not particularly interesting to calculate these Fourier coefficients, since the most straightforward way to obtain F_{ts} is to measure directly $q(t)$ or its spectrum and employ equation (B.3). No further approximations are necessary in this case and F_{ts} can be fully reconstructed along the sampled path.

In the *harmonic approximation*, the deflection is approximated by equation (4) and the tip-sample force is accordingly approximated as

$$F_{\text{ts}}(t) = F_{\text{even}}^{(0)} + F_{\text{even}}^{(1)} \cos(2\pi \nu_{\text{exc}} t + \varphi) + F_{\text{odd}}^{(1)} \sin(2\pi \nu_{\text{exc}} t + \varphi) \quad (\text{C.11})$$

while equations (C.6)–(C.8) remain valid. In this case, the physical meaning of the Fourier coefficients becomes obvious

$$F_{\text{even}}^{(0)} = \langle F_{\text{even}} \rangle_{\cup} \quad (\text{C.12})$$

$$F_{\text{even}}^{(1)} = A \langle k_{\text{ts}} \rangle_{\cap} \quad (\text{C.13})$$

$$F_{\text{odd}}^{(1)} = (2\pi \nu_{\text{exc}}) A \langle \gamma_{\text{ts}} \rangle_{\cap} \quad (\text{C.14})$$

since $\langle k_{\text{ts}} \rangle_{\cap}$ is the average tip-sample force gradient and $\langle \gamma_{\text{ts}} \rangle_{\cap}$ is the average tip-sample damping constant. Within the harmonic approximation, it is a feasible approach to obtain F_{even} from a deconvolution of $\langle k_{\text{ts}} \rangle_{\cap}$ and F_{odd} from a deconvolution of $\langle \gamma_{\text{ts}} \rangle_{\cap}$ if both quantities are velocity-independent.

Appendix D. Convolution and deconvolution

In this section we discuss the convolution of F_{even} , k_{ts} and γ_{ts} into $\langle F_{\text{even}} \rangle_{\cup}$, $\langle k_{\text{ts}} \rangle_{\cap}$ and $\langle \gamma_{\text{ts}} \rangle_{\cap}$ as well as the inverse operation, the deconvolution. We employ the harmonic approximation, which means the path of the tip is given by the deflection and velocity as expressed in equation (4).

First, we convert each time-average introduced in equations (8), (11) and (14) into a convolution, i.e. a weighted average over the tip-sample distance. Using equation (20), the time-average of F_{even} can be written as

$$\begin{aligned}
 \langle F_{\text{even}}(z_{\text{ts}}, \dot{z}_{\text{ts}}) \rangle_t &= \lim_{T \rightarrow \infty} \frac{1}{2T} \int_{-T}^T dt F_{\text{even}}(z_c + A \cos(2\pi\nu_{\text{exc}}t + \varphi), \dot{z}_{\text{ts}}) \\
 &= \frac{1}{\pi} \int_0^\pi d\theta F_{\text{even}}(z_c + A \cos \theta, \dot{z}_{\text{ts}}) \\
 &= \int_{-A}^A dz F_{\text{even}}(z_c + z, \dot{z}_{\text{ts}}) \frac{1}{\pi\sqrt{A^2 - z^2}} \\
 &= \langle F_{\text{even}}(z_{\text{ts}}, \dot{z}_{\text{ts}}) \rangle_{\cup}.
 \end{aligned} \tag{D.1}$$

From the time-average of $F_{\text{even}} \cdot (z_{\text{ts}} - z_c)$ we obtain the following convolution of the tip-sample force gradient k_{ts} :

$$\begin{aligned}
 \langle F_{\text{even}}(z_{\text{ts}}, \dot{z}_{\text{ts}}) \cdot (z_{\text{ts}} - z_c) \rangle_t &= A \lim_{T \rightarrow \infty} \frac{1}{2T} \int_{-T}^T dt \\
 &\quad \cdot F_{\text{even}}(z_c + A \cos(2\pi\nu_{\text{exc}}t + \varphi), \dot{z}_{\text{ts}}) \\
 &\quad \cdot \cos(2\pi\nu_{\text{exc}}t + \varphi) \\
 &= \frac{A}{\pi} \int_0^\pi d\theta F_{\text{even}}(z_c + A \cos \theta, \dot{z}_{\text{ts}}) \cos \theta \\
 &= \frac{1}{\pi} \int_{-A}^A dz F_{\text{even}}(z_c + z, \dot{z}_{\text{ts}}) \\
 &\quad \cdot \frac{z}{\sqrt{A^2 - z^2}} \\
 &= \frac{A^2}{2} \int_{-A}^A dz \frac{\partial F_{\text{even}}(z_c + z, \dot{z}_{\text{ts}})}{\partial z} \\
 &\quad \cdot \frac{2}{\pi A^2} \sqrt{A^2 - z^2} \\
 &= \frac{A^2}{2} \langle k_{\text{ts}}(z_{\text{ts}}, \dot{z}_{\text{ts}}) \rangle_{\cap}.
 \end{aligned} \tag{D.2}$$

Here, we made use of equation (2), the definition of the cap-average in equation (21) and the definition of the tip-sample force gradient according to equation (15). From the time-average of $F_{\text{odd}} \cdot \dot{z}_{\text{ts}}$ we obtain the following convolution of the tip-sample damping constant γ_{ts} :

$$\begin{aligned}
 \langle F_{\text{odd}}(z_{\text{ts}}, \dot{z}_{\text{ts}}) \cdot \dot{z}_{\text{ts}} \rangle_t &= - \lim_{T \rightarrow \infty} \frac{1}{2T} \int_{-T}^T dt \\
 &\quad \cdot \gamma_{\text{ts}}(z_c + A \cos(2\pi\nu_{\text{exc}}t + \varphi), \dot{z}_{\text{ts}}) \cdot (\dot{z}_{\text{ts}})^2 \\
 &= - \frac{(2\pi\nu_{\text{exc}}A)^2}{\pi} \int_0^\pi d\theta \\
 &\quad \cdot \gamma_{\text{ts}}(z_c + A \cos \theta, \dot{z}_{\text{ts}}) \sin^2 \theta \\
 &= - \frac{(2\pi\nu_{\text{exc}}A)^2}{2} \int_{-A}^A dz \gamma_{\text{ts}}(z_c + z, \dot{z}_{\text{ts}}) \\
 &\quad \cdot \frac{2}{\pi A^2} \sqrt{A^2 - z^2} \\
 &= - \frac{(2\pi\nu_{\text{exc}}A)^2}{2} \langle \gamma_{\text{ts}}(z_{\text{ts}}, \dot{z}_{\text{ts}}) \rangle_{\cap}.
 \end{aligned} \tag{D.3}$$

In the above equation, we used equations (3) and (21) as well as the definition of the tip-sample damping constant according to equation (16).

The weighted average in equation (D.1) is a convolution of F_{even} with w_{\cup} (equation (20), figure D1(a)). The weighted

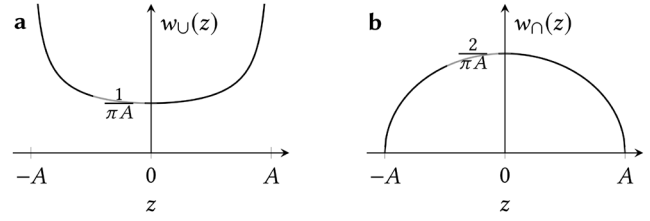


Figure D1. Plot of the weight functions *cup* (a) and *cap* (b) that are used to average the quantities F_{even} as well as k_{ts} and γ_{ts} , respectively. Both weight functions are normalized, meaning that an integral of the weight function from $-A$ to A equals one.

averages obtained in equations (D.2) and (D.3) are convolutions of k_{ts} and γ_{ts} with w_{\cap} (equation (21), figure D1(b)). The inverse operation needed for extracting k_{ts} , γ_{ts} and F_{even} from the weighted averages is the *deconvolution*. Different numerical recipes have been proposed for the deconvolution of the cup-average and the cap-average [9, 27–29]. Here, we have chosen to reproduce the result originally obtained by Sader *et al* [28, 29], which has been described in numerous works [19–21, 26]. The procedure is described in the following. We first start by motivating the general idea:

When the tip is not interacting with the sample (at distance z_{∞}), F_{ts} is zero over the entire path probed by the tip. Consequently, all three averages are zero as well. This is usually the case if the tip is far away from the sample. When the tip is gradually approached to the sample, at some point it will start to probe along a path where the tip-sample force is not always zero. The non-zero F_{ts} gives rise to a change in the three averages that arises from the part of the path that has not been sampled before. Obtaining averages for various, yet partly overlapping paths is the basis for deconvolution. There are several possibilities for finding sufficiently overlapping paths: Typically, the z -piezo displacement z_p is varied in the experiment to change the tip-sample distance. In this approach, the excitation parameters (F_0 , ν_{exc}) and the observables (q_s , A , φ) are recorded as function of z_p . Using the AFM equations (22)–(24) allows to extract the average of k_{ts} , γ_{ts} and F_{even} as a function of the center position of the tip $z_c = z_0 + z_p + q_s$. The dependence of the average on the center position is indicated with the notation $\langle f \rangle_{\cup}^{(z_c)}$ and $\langle f \rangle_{\cap}^{(z_c)}$, respectively.

While convolution is always possible, deconvolution requires to impose further conditions. The convolution equations (D.1)–(D.3) represent weighted averages along the tip-sample distance interval probed by the tip, although F_{even} , k_{ts} and γ_{ts} are in general velocity dependent. The convolutions are possible, because all three quantities are even with respect to velocity and, therefore, unique functions of the tip-sample distance as discussed in section 2. The latter is only true on the specific path described by equation (4). For a deconvolution along the tip-sample distance, we additionally require the quantities F_{even} , k_{ts} and γ_{ts} to be *unique* functions of the tip-sample distance *in the entire* z_{ts} *interval* probed by the tip during the measurement. Otherwise there would be no sufficient overlap of the paths. This criterion is only fulfilled if F_{even} , k_{ts} and γ_{ts} do not depend on the tip velocity.

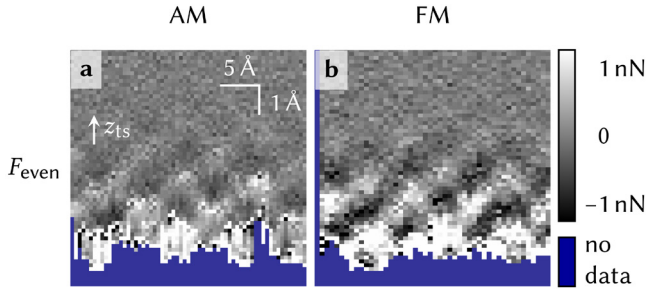


Figure D2. The even contribution of the tip-sample force obtained by deconvolution of the averaged tip-sample force gradient and subsequent integration. Data in (a) results from AM-AFM data (figure 4(c)), data in (b) from FM-AFM data (figure 4(d)). The vertical axis corresponds to the tip-sample distance z_{ts} . As in figure 4, the horizontal axis corresponds to the lateral [48 $\bar{1}$] direction of the calcite (10.4) surface. The color bar applies to both data sets.

The following two equations for the deconvolution have been derived: [28, 29]

$$f(z_c - A) = \langle f \rangle_{\cup}^{(z_c)} - \int_{z_c - A}^{z_c} \left[\sqrt{\frac{2A}{z - (z_c - A)}} \left(\frac{d\langle f \rangle_{\cup}^{(z)}}{dz} - \sqrt{\frac{2}{\pi}} \frac{d\langle f \rangle_{\cup}^{(z+A)}}{dz} \right) \right] dz \quad (D.4)$$

$$f(z_c - A) = -\frac{\partial}{\partial z_c} \int_{z_c - A}^{z_c} \left[\left(1 + \sqrt{\frac{A}{64\pi(z - (z_c - A))}} \right) \langle f \rangle_{\cap}^{(z)} - \sqrt{\frac{A^3}{2(z - (z_c - A))}} \frac{\partial \langle f \rangle_{\cap}^{(z)}}{\partial z} \right] dz. \quad (D.5)$$

Note that the even contribution to the tip-sample force F_{even} can either be obtained by deconvolving the cup average $\langle F_{\text{even}} \rangle_{\cup}$ according to equation (D.4) or by deconvolving the cap-averaged tip-sample force gradient $\langle k_{ts} \rangle_{\cap}$ according to equation (D.5) and subsequent integration along z_c .

As demonstration, we obtained the even contribution F_{even} by deconvolution and subsequent integration of the averaged tip-sample force gradient shown in figure 4(c) and (d) with the following equation [39] that can be used for N discrete data points with spacing Δz .

$$F_{\text{even}}(z_k) = -\langle k_{ts} \rangle_{\cap}^{(z_k)} \Delta z - \sqrt{\frac{A}{16\pi}} \langle k_{ts} \rangle_{\cap}^{(z_k)} \sqrt{\Delta z} + \sqrt{\frac{4A^3}{2}} \frac{\langle k_{ts} \rangle_{\cap}^{(z_{k+1})} - \langle k_{ts} \rangle_{\cap}^{(z_k)}}{\sqrt{\Delta z}} - \sum_{i=k+1}^{N-1} \left[\left(1 + \sqrt{\frac{A}{64\pi(z_i - z_k)}} \right) \langle k_{ts} \rangle_{\cap}^{(z_i)} - \sqrt{\frac{A^3}{2(z_i - z_k)}} \frac{\langle k_{ts} \rangle_{\cap}^{(z_{i+1})} - \langle k_{ts} \rangle_{\cap}^{(z_i)}}{\Delta z} \right] \Delta z. \quad (D.6)$$

The first three terms in the above equation (without the summation bracket) are correction terms first introduced in the by now unavailable Mathematica notebook by Sader and Jarvis

[28] and reproduced in [39] (the code we used for the deconvolution according to the above equation is available from the first author). The resulting even contribution to the tip-sample force F_{even} is shown in figure D2. Both datasets show similar features, however, F_{even} is not quantitatively equal. A possible explanation for the discrepancy could be that F_{even} depends on the tip-velocity. Accordingly, the requirement for the deconvolution of F_{even} being a unique function of z_{ts} along the full tip-sample distance interval probed by the tip would not be fulfilled.

Appendix E. Prevalent, yet restrictive approximations in FM-AFM

In the literature reporting FM-AFM data analysis [5, 6], the following approximations of the AFM equations are often found:

$$\langle F_{\text{even}}(z_{ts}, \dot{z}_{ts}) \rangle_t = kq_s \approx 0 \quad (E.1)$$

$$\langle k_{ts}(z_{ts}, \dot{z}_{ts}) \rangle_{\cap} = k \left(1 - \left(\frac{\nu_{\text{exc}}}{\nu_e} \right)^2 \right) - \frac{F_0}{A} \cos \varphi \approx -2k \frac{\nu_{\text{exc}} - \nu_e}{\nu_e} \quad (E.2)$$

$$\langle \gamma_{ts}(z_{ts}, \dot{z}_{ts}) \rangle_{\cap} = -\frac{k}{2\pi\nu_e Q} - \frac{F_0}{2\pi\nu_{\text{exc}} A} \sin \varphi \approx \frac{k}{2\pi\nu_e Q} \left(\frac{F_0}{F_0(F_s = 0)} - 1 \right). \quad (E.3)$$

Here, several restrictions and approximations have been employed:

- The static deflection q_s is negligible.
- Both FM-AFM feedback loops are working ideally and, thus, the amplitude is assumed to be exactly the amplitude setpoint and the phase shift is assumed to be exactly $-\pi/2$.
- The difference between excitation frequency and eigenfrequency $\nu_{\text{exc}} - \nu_e$ (referred to as ‘frequency shift’ or ‘detuning’) is small compared to ν_e (for equation (E.2)) or negligible (for equation (E.3)).

These approximations are not always justified. The magnitude of the static deflection q_s can be significant in both ultra-high vacuum [23] as well as in liquid environment [32]. Relying on ideally working feedback loops is an unnecessary limitation since the AFM equations can handle any AFM data irrespective of how well the employed feedback loops (if any) work. The excitation frequency can differ significantly from the eigenfrequency. In the data presented in figure 4(a) for example, the excitation frequency reaches values of up to $1.2\nu_e$. Therefore, we recommend using the three AFM equations (22)–(24) instead of the approximated equations (E.1)–(E.3).

Appendix F. Experimental method

For the experiments we used a modified commercial AFM [36] equipped with photothermal excitation [37] in combination with a customized data acquisition system [38]. Experimental details regarding the sample and cantilever as well as the operation in the FM mode are described in [38]. For operation in the AM mode, we set $\nu_{\text{exc}} \approx 0.95\nu_e$ and $F_0 = 0.6$ nN. When performing AM-AFM, the closest approach to the sample was limited to the position where the amplitude A decreased to 0.1 of the amplitude of the retracted cantilever. For FM-AFM, the closest approach was limited to the position where $\nu_{\text{exc}} > 1.2\nu_e$. The data is plotted as a function of z_c , the center position of the tip oscillation. The datasets were arbitrarily aligned at the averaged position of closest approach.

References

- [1] Binnig G, Quate C F and Gerber C 1986 *Phys. Rev. Lett.* **56** 930
- [2] Martin Y, Williams C C and Wickramasinghe H K 1987 *J. Appl. Phys.* **61** 4723
- [3] Nishi R, Houda I, Aramata T, Sugawara Y and Morita S 2000 *Appl. Surf. Sci.* **157** 332
- [4] Albrecht T R, Grütter P, Horne D and Rugar D 1991 *J. Appl. Phys.* **69** 668
- [5] Giessibl F J 1997 *Phys. Rev. B* **56** 16010
- [6] Giessibl F J 2003 *Rev. Mod. Phys.* **75** 949
- [7] Dürig U 1999 *Appl. Phys. Lett.* **75** 433
- [8] Dürig U 1999 *Surf. Interface Anal.* **27** 467
- [9] Dürig U 2000 *Appl. Phys. Lett.* **76** 1203
- [10] Dürig U 2000 *New J. Phys.* **2** 5
- [11] Sasaki N, Tsukada M, Tamura R, Abe K and Sato N 1998 *Appl. Phys. A* **66** 287
- [12] Sasaki N and Tsukada M 1998 *Japan. J. Appl. Phys.* **37** 533
- [13] Sasaki N and Tsukada M 1999 *Appl. Surf. Sci.* **140** 339
- [14] Sasaki N and Tsukada M 2000 *Japan. J. Appl. Phys.* **39** 1334
- [15] Hölscher H 2006 *Appl. Phys. Lett.* **89** 123109
- [16] Hölscher H and Schwarz U D 2007 *Int. J. Nonlinear Mech.* **42** 608
- [17] Hölscher H 2008 *J. Appl. Phys.* **103** 064317
- [18] Ebeling D and Hölscher H 2007 *J. Appl. Phys.* **102** 114310
- [19] Payam A F, Martin-Jimenez D and Garcia R 2015 *Nanotechnology* **26** 185706
- [20] Katan A J, van Es M H and Oosterkamp T H 2009 *Nanotechnology* **20** 165703
- [21] Sader J E, Uchihashi T, Higgins M J, Farrell A, Nakayama Y and Jarvis S P 2005 *Nanotechnology* **16** 94
- [22] Green E I 1955 *Am. Sci.* **43** 584
- [23] Kawai S, Glatzel T, Koch S, Such B, Baratoff A and Meyer E 2009 *Phys. Rev. B* **80** 085422
- [24] Cleveland J P, Anczykowski B, Schmid A E and Elings V B 1998 *Appl. Phys. Lett.* **72** 2613
- [25] Hölscher H, Gotsmann B, Allers W, Schwarz U D, Fuchs H and Wiesendanger R 2001 *Phys. Rev. B* **64** 075402
- [26] Suzuki K, Kobayashi K, Labuda A, Matsushige K and Yamada H 2014 *Appl. Phys. Lett.* **105** 233105
- [27] Giessibl F J 2001 *Appl. Phys. Lett.* **78** 123
- [28] Sader J E and Jarvis S P 2004 *Appl. Phys. Lett.* **84** 1801
- [29] Sader J E and Sugimoto Y 2010 *Appl. Phys. Lett.* **97** 043502
- [30] Kawai S, Federici Canova F F, Glatzel T, Foster A S and Meyer E 2011 *Phys. Rev. B* **84** 115415
- [31] Imada H, Kimura K and Onishi H 2013 *Langmuir* **29** 10744
- [32] Marutschke C, Walters D, Cleveland J, Hermes I, Bechstein R and Kühnle A 2014 *Nanotechnology* **25** 335703
- [33] Araki Y, Tsukamoto K, Takagi R, Miyashita T, Oyabu N, Kobayashi K and Yamada H 2014 *Cryst. Growth Des.* **14** 6254
- [34] Fukuma T, Reischl B, Kobayashi N, Spijker P, Canova F F, Miyazawa K and Foster A S 2015 *Phys. Rev. B* **92** 155412
- [35] Söngen H, Marutschke M, Spijker P, Holmgren E, Hermes I, Bechstein R, Klassen S, Tracey J, Foster A S and Kühnle A 2017 *Langmuir* **33** 125
- [36] Rode S, Stark R, Lübbe J, Tröger L, Schütte J, Umeda K, Kobayashi K, Yamada H and Kühnle A 2011 *Rev. Sci. Instrum.* **82** 73703
- [37] Adam H, Rode S, Schreiber M, Kobayashi K, Yamada H and Kühnle A 2014 *Rev. Sci. Instrum.* **85** 23703
- [38] Söngen H, Nalbach M, Adam H and Kühnle A 2016 *Rev. Sci. Instrum.* **87** 063704
- [39] Kuhn S, Kittelmann M, Sugimoto Y, Abe M, Kühnle A and Rahe P 2014 *Phys. Rev. B* **90** 195405